Symmetric Inertial-Confinement-Fusion-Capsule Implosions in a Double-Z-Pinch-Driven Hohlraum

G. R. Bennett,[1] M. E. Cuneo,[2] R. A. Vesey,[2] J. L. Porter,[2] R. G. Adams,[2] R. A. Aragon,[2] J. A. Caird,[3] O. L. Landen,[3] P. K. Rambo,[2] D. C. Rovang,[2] L. E. Ruggles,[2] W. W. Simpson,[2] I. C. Smith,[2] and D. F. Wenger[2]

[1]*Ktech Corporation, 2201 Buena Vista SE, Suite 400, Albuquerque, New Mexico 87106-4265*
[2]*Sandia National Laboratories, P.O. Box 5800, Albuquerque, New Mexico 87185-1193*
[3]*Lawrence Livermore National Laboratory, P.O. Box 808, Livermore, California 94551*

(Received 3 June 2002; published 26 November 2002)

An inertial-confinement-fusion (ICF) concept using two 60-MA Z pinches to drive a cylindrical hohlraum to 220 eV has been recently proposed. The first capsule implosions relevant to this concept have been performed at the same physical scale with a lower 20-MA current, yielding a 70 ± 5 eV capsule drive. The capsule shell shape implies a polar radiation symmetry, the first high-accuracy measurement of this type in a pulsed-power-driven ICF configuration, within a factor of 1.6–4 of that required for scaling to ignition. The convergence ratio of 14–21 is to date the highest in any pulsed-power ICF system.

DOI: 10.1103/PhysRevLett.89.245002 PACS numbers: 52.59.Qy, 52.57.Fg, 52.58.Lq

In the hot-spot ignition approach to indirect drive inertial confinement fusion (ICF), a spherical capsule containing cryogenic deuterium-tritium (DT) fuel is uniformly compressed by intense Planckian x-ray radiation to high temperature and density [1]. The temporal profile of the radiation temperature is designed so that the majority of the fuel is imploded along a low entropy adiabat, and a high-temperature low-density hot spot (created by coalescing shocks at the center) of low fuel mass surrounded by cool, high density DT is attained. With a sufficiently high ion temperature $T_{\rm ion}$ and areal density at the hot spot, 3.56 MeV α particles from the $\mathrm{D} + \mathrm{T} \rightarrow n + \alpha$ reaction are produced and then slowed. By depositing kinetic energy along their path, the α particles bootstrap $T_{\rm ion}$ up to 60 keV, thus initiating a radially propagating burn wave in the main fuel region, leading to ignition. The radiation field must be sufficiently uniform to drive the capsule to high convergence with minimal shell distortion. Such fields are contained by a high-Z radiation case, or hohlraum, and can be generated by, for example, multiple laser beam irradiation of the cavity wall [1]. Recently, a high-yield (HY) double-Z-pinch-driven hohlraum ICF concept has been proposed [2] that shares some similarities to the laser-driven cylindrical hohlraum ICF approach. Here, two axially located Z pinches at either end of a cylindrical "secondary" hohlraum, each driven by a separate 60-MA power feed, replace the laser beams as the energy source, creating a 220 eV hohlraum radiation temperature.

In this Letter, ICF capsule implosions and polar radiation symmetry measurements at 70 ± 5 eV in a 20-MA, single-power feed variant (but same physical scale) of this high-yield double-Z-pinch-driven hohlraum concept [3–5], on Sandia National Laboratories's Z accelerator [6], are reported for the first time. These represent the first capsule implosions in a Z-pinch-driven hohlraum with a fixed wall, and the high-accuracy polar radiation symmetry measurement is the first in a pulsed-power-driven ICF configuration. The measured polar radiation symmetry in an initial computer-optimized hohlraum was within a factor of 1.6–4 of that required to scale to ignition and HY. The capsule-convergence ratio (Cr) in a deliberately nonoptimized hohlraum was $\mathrm{Cr} = 14$–21, the highest yet demonstrated in a pulsed-power-driven ICF system. In this work, the double-pinch hohlraum exhibits time-averaged radiation drive asymmetries, $\langle \Delta I \rangle / I$ [3,7], at the capsule, that are sufficiently low to be of near-term interest in the U.S. ICF program; i.e., $\langle \Delta I \rangle / I = 6 \pm 1$ [%] at the 70 ± 5 eV (FW84%M = 13–16 ns, full-width at 84% maximum) capsule drive temperature on Z. While this drive uniformity is not at the ignition-relevant requirement of $\langle \Delta I \rangle / I = 0.73\%$ [3,8], detailed simulations indicate that the increased hohlraum wall albedo α at the higher, HY-relevant 220 eV (FW84%M = 12.5 ns) capsule drive would scale the measured $\langle \Delta I \rangle / I$ to reduced levels; i.e., 1.2%–2.9% (within a factor of 1.6–4 of 0.73%). These calculations include the effects of the different case-to-capsule ratios in the HY design and the current implosions.

In the high-yield concept relevant to these experiments, each axial Z pinch is located within a separate primary hohlraum at either end of the central secondary hohlraum containing the 5-mm diameter cryogenic fusion capsule [Fig. 1(a)]. Upon stagnation, kinetic and magnetic energy is efficiently converted to x rays, thus creating, after thermalization, near-Planckian radiation fields in the secondary and both primary hohlraums [4]. With an overlap of reemission radiation from both primaries and the secondary hohlraum walls, the capsule is driven by a 220 eV radiation temperature with a flux uniformity dependent on the primary and secondary hohlraum

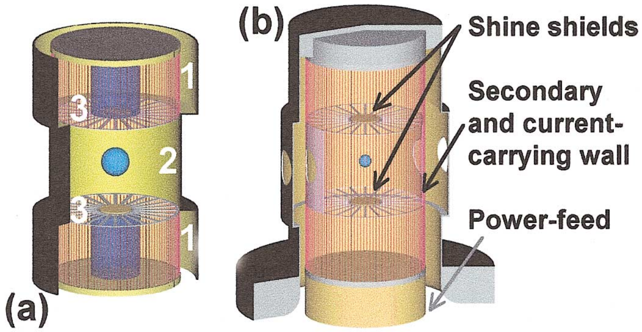

FIG. 1 (color). (a) High-yield dual power-feed double-Z-pinch-driven hohlraum ICF driver configuration, where each Z pinch is powered by a 60-MA current. Direct pinch emission and reemission from the primary hohlraum wall [1] flow into the secondary hohlraum [2] through a beryllium return-current array [3]. (b) The Z accelerator 20-MA, single power-feed variant is at a similar physical scale.

geometry, with little sensitivity to mm-scale-length structure in the pinch emission [2,9–11]. On the Z accelerator, the recently developed single-power feed variant of this geometry (the advanced, glueless load design [3]), at the same physical size [3–5], drove the capsule implosions reported here with a 70 ± 5 eV radiation temperature. In this case [Fig. 1(b)], electrical power enters through a single 3-mm anode-cathode gap in the lower primary hohlraum and current runs the outside length of the secondary hohlraum to drive the upper pinch. Both pinches are 10-mm in length and are formed from a single tungsten wire array [3].

To attain modest convergence with sufficient shell stability in the 70 ± 5 eV drive field on Z, 2.15-mm diameter glow discharge polymer plastic capsules of 59-μm wall thickness and 0.85-mg wall mass were used. With a 1 ATM air gas fill, the calculated peak convergence ratio based on the gas cavity boundary was 23 at the 75 eV upper level of the drive temperature. Each capsule was mounted between two vertical (or horizontal) 0.35-μm thick formvar ($C_5H_8O_2$ at 1.19 gm/cc) layers, and the target was radiographed normal to the z axis of the cylindrical symmetry.

Point projection x-ray imaging with the Z-Beamlet Laser (ZBL) [12] system provided the capsule implosion diagnostic [13]. With a 140 μm FWHM Gaussian x-ray spot (600 ps FWHM laser pulse width), the 4.8× magnification point projection imaging scheme provided a single 6.7 keV (predominantly Fe He$_\alpha$) x-ray image of the imploding capsule with 120–150 μm spatial resolution, over a 3-mm diameter field of view. The 6.7 keV backlighting energy was chosen because it provided good shell contrast over a wide capsule-convergence ratio range. Two time-resolved transmission-grating spectrometers measured the upper and lower primary hohlraum temperatures ($\pm 5\%$ measurement error for each primary) on selected shots [3–5].

The secondary hohlraum length and shine shield diameter were optimized (using power balance inferred on shot Z766 [3]) to provide the most symmetric time-averaged capsule polar radiation drive using a 2D time-dependent radiation view factor code OPTSEC [9,10]. The fixed primary hohlraum geometry and the fixed secondary hohlraum diameter provided the optimization constraints. Because of the hohlraum cylindrical symmetry, the radiation drive can be expressed in terms of Legendre polynomials, P_n. The P_2 to P_8 even mode Legendre polynomials were minimized when averaged over the drive pulse with a 15.6-mm length, 18.476-mm inside diameter, and 6.5-mm diameter shine shields. Using the measured upper and lower primary hohlraum temperatures on shot Z829 (slight nonideal pinch balance throughout the drive), OPTSEC inferred the time-integrated radiation flux asymmetry to be $\langle \Delta I \rangle / I = 2.8\%$ (or 1.9% for "best center" asymmetry, discussed later), with a peak secondary temperature of 68 ± 4 eV.

Figure 2(a) displays a typical capsule preshot radiograph, and Fig. 2(b) shows the Z830 capsule implosion image taken 10 ± 1.3 ns after peak primary radiation temperature. For comparison, Fig. 2(c) is shot Z837 (discussed later) captured at 22.5 ± 1.3 ns in an nonoptimized hohlraum. For Z830, the initial to final radii of minimum shell transmission, Cr, is 1.83 ± 0.04. Figure 3 plots the capsule's right-hand side (rhs) radius of minimum transmission as a function of polar angle (in Fig. 3 the 0° point is the capsule bottom; for clarity, error bars are shown for only every 30° increment). Also plotted is the result of a 2D LASNEX [14] simulation using as input the OPTSEC-inferred 2D time-dependent drive asymmetry and drive temperature from shot Z829. The relevant a_1-a_4 coefficients are listed, along with an error estimate from changing the two primary temperatures by 2.5% in opposite directions (i.e., +2.5% on upper primary and −2.5% on lower, and vice versa). The Legendre

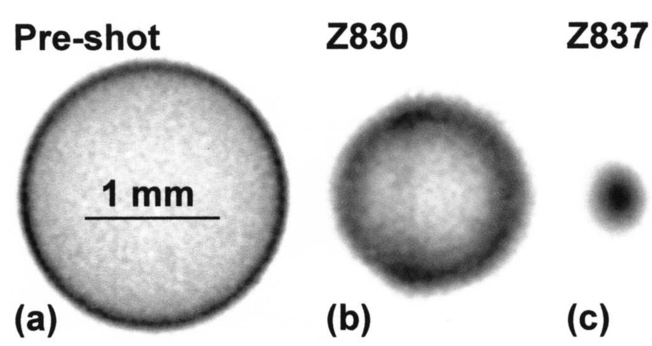

FIG. 2. (a) Preshot radiograph of a typical capsule. (b) Z830 capsule implosion image at 6.7 keV taken at 10 ± 1.3 ns after peak primary radiation temperature. (c) Capsule implosion Z837 image (also at 6.7 keV) in a "nonoptimized" hohlraum captured at 22.5 ± 1.3 ns. Although distorted, it is an example of moderate convergence.

coefficient a_0 of the simulated result was adjusted slightly to allow a clearer comparison between the dominant mode features. Also note the capsule left-hand side is not included in Fig. 3 because a faint axial feature overlies that side of the capsule [see Fig. 2(b)] and interferes with the analysis. However, because of cylindrical symmetry in the hohlraum geometry it is sufficient here to study only the rhs. The axial feature was caused by having apertures in current-carrying surfaces, but was reduced on later shots (e.g., Z837 [Fig. 2(c)] and Z839 [Fig. 4]) by applying thin mylar windows over the backlighter apertures.

The image analysis plotted in Fig. 3 indicates that $\langle \Delta r \rangle / r$ [3,15], the shell distortion from sphericity, is 4.4 ± 0.8 [%], corresponding to deflections of 25 μm, within the 10% limit of the 120–150 μm spatial resolution that an interference can generally be tracked. An 18th order Legendre polynomial fit, with the a_1-a_8 coefficients listed in Fig. 3, also gives $\langle \Delta r \rangle / r = 4.4 \pm 0.8$ [%]. The center around which r is defined is not the original capsule center, since a finite P_1 undoubtedly occurred; rather, it is the best center where the sum of $r(\theta)\cos(\theta)$ and the sum of $r(\theta)\sin(\theta)$ are simultaneously minimized. To infer the resultant drive asymmetry, the relation [3,8]

$$\langle \Delta r \rangle / r = (7/8)(\langle \Delta I \rangle / I)(\mathrm{Cr} - 1) \qquad (1)$$

is used. $\langle \Delta I \rangle / I$ is as defined earlier [7] except now using the best center of the drive asymmetry. Detailed 2D LASNEX simulations indicate that Eq. (1) is reasonably accurate, throughout the Cr range considered here, for any particular low mode drive asymmetry spectrum of *sufficiently* small amplitude; e.g., from a pure P_1 to a more complex combination of P_1, P_2, P_3, and P_4. (In the case of a pure even mode asymmetry, the best center of $\langle \Delta r \rangle / r$ and $\langle \Delta I \rangle / I$ is the original origin.) Therefore, using $\langle \Delta r \rangle / r = (7/8)(\langle \Delta I \rangle / I)(\mathrm{Cr} - 1)$ where $\mathrm{Cr} = 1.83 \pm 0.04$ and $\langle \Delta r \rangle / r = 4.4 \pm 0.8$ [%], the inferred drive asymmetry (best center) is $\langle \Delta I \rangle / I = 6.1 \pm 1.1$ [%]. With a respective factor of 2.8 and 1.38 reduction in even and odd mode drive asymmetry at the 220 eV ignition-relevant temperature [3], it is possible to determine the effective high-yield drive asymmetry, as follows: Given that $\langle \Delta r \rangle / r$ and $\langle \Delta I \rangle / I$ are linearly related, then the Legendre polynomial fit coefficients can be scaled by a factor of $1/2.8$ (even) and $1/1.38$ (odd). As a result $\langle \Delta r \rangle / r$ is reduced to 2.1%, thus implying $\langle \Delta I \rangle / I = 2.9\%$, which is a factor of 4 of the high-yield requirement of 0.73% [3,8]. If a perfect power balance for the dual-power feed is also considered, then the odd mode shell distortion coefficients would be zero (the even mode coefficients would change very slightly). In this case $\langle \Delta r \rangle / r = 0.9\%$, implying $\langle \Delta I \rangle / I = 1.2\%$; i.e., a factor of 1.6 of the HY requirement. Given that a dual power feed may not necessarily guarantee ideal power balance, however, the Z830 inferred drive symmetry can be best described as being within a factor of 1.6–4 of that required for HY.

On the basis of this analysis, the "optimum" secondary hohlraum geometry clearly requires additional optimization through further experimentation and modeling to meet the HY symmetry-scaling requirement. (In this pursuit, improved x-ray backlighter imaging spatial resolution of the capsule, possibly using advanced laser-backlit grazing-incidence imaging systems for the very highest spatial resolution at much higher Cr [16,17], is required.) However, it is encouraging that such low shell distortions were measured, and a highly uniform drive was inferred, in these initial experiments.

Figure 4 shows a plot of the average radius of minimum transmission for Z830 and Z831 (68 ± 4 eV), Z839 (72 ± 4 eV), and Z833 (75 ± 4 eV) with the corresponding 1D LASNEX predictions at the relevant drive temperatures (and accounting for the 140-μm FWHM Gaussian x-ray spot). Bearing in mind the ± 4 eV uncertainty in the measured drive, the close agreement here between

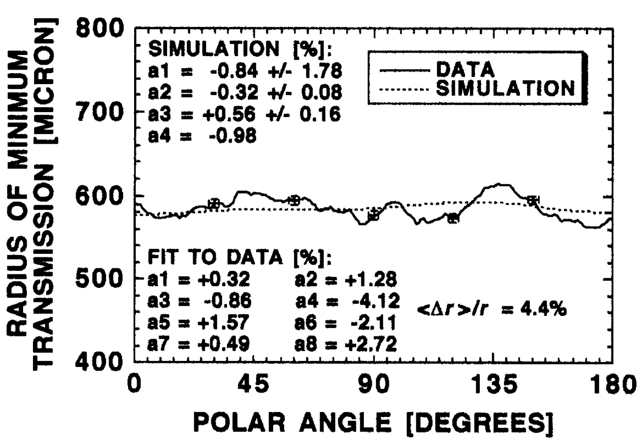

FIG. 3. Radius of minimum transmission vs polar angle for the right-hand side of the Z830 capsule, compared with simulation. The first eight coefficients of an 18th order Legendre polynomial fit to the data are shown.

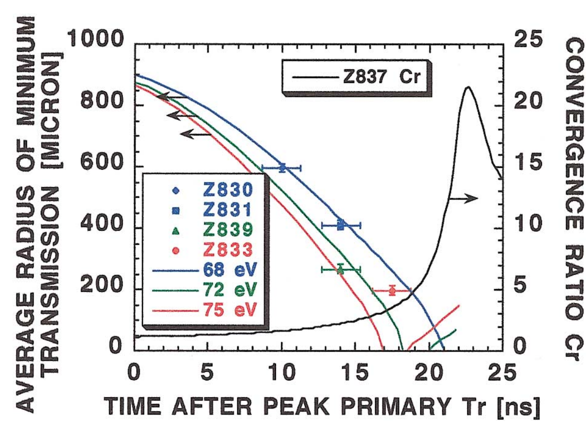

FIG. 4 (color). Z837 capsule convergence ratio vs time and average radius of minimum transmission vs time trajectory for other shots.

simulation and data confirms previous measurements and models of hohlraum energetics and secondary coupling [4,5] and suggests that the first order capsule physics is well understood. Z837 [Fig. 2(c)], captured at 22.5 ± 1.3 ns, was driven in a shorter, 13.0-mm length, but otherwise identical secondary hohlraum to Z830. Although the hohlraum geometry was deliberately not the optimum (part of a geometric symmetry control study to be reported in a later publication), evident in the ''equator-hot'' core shape, the capsule reached a moderate convergence. The measured Z837 primary temperatures were postprocessed in OPTSEC to provide input to a 2D LASNEX capsule simulation. With a 67.6 eV peak capsule drive temperature, the simulated capsule reaches a peak convergence ratio (based on gas cavity volume) of $\mathrm{Cr} = 21.6$ at 22.7 ns, as shown in Fig. 4. The same simulation predicts a polar averaged peak shell density of 38 g/cm^3 and a polar averaged peak shell areal density of 0.24 g/cm^3.

To infer the Z837 [Fig. 2(c)] convergence ratio, horizontal and vertical lineouts of backlighter x-ray transmission (T) through the capsule were extracted. The $T = 0.5$ points were assigned asymmetric transmission error bars of 0 to -0.1, i.e., $T = 0.5$–0.4. These asymmetric error bars were the result of hole-closure plasma, from the primary and secondary hohlraum backlighter apertures [Fig. 1(b)], creating a nonflat, approximately linear backlighter flux that (without correction) tended to increase the apparent capsule transmission as the center was approached. Future experiments will attempt to eliminate completely these hole-closure plasma issues. The measured profiles were then overlaid onto the horizontal and vertical synthetic transmission profiles from the 2D LASNEX simulation (backlit with the 140-μm FWHM Gaussian x-ray spot). At a time of 22.3 ns the simulation simultaneously best matches the FWHMs of the horizontal and vertical profile data, and thus the equator-hot capsule shape. However, since a 0 to -0.1 transmission error bar has been assigned, it is equally important to determine the best fit to the same displacement points but at a transmission of 0.4. The horizontal and vertical synthetic profiles best match this point at 21.6 ns. Likewise, the simulation best matches the $T = 0.45$ point at 21.9 ns. At these times, all within the measured 22.5 ± 1.3 ns timing interval, the convergence ratios are $\mathrm{Cr} = 20.8$ at 22.3 ns; $\mathrm{Cr} = 14.2$ at 21.6 ns; and $\mathrm{Cr} = 17.1$ at 21.9 ns. Thus, the convergence ratio of Z837 is inferred to be $\mathrm{Cr} = 14$–21.

In conclusion, ICF capsule implosions and polar radiation symmetry measurements at 70 ± 5 eV in a 20-MA, single-power feed variant of the 220 eV, 60-MA, dual-power feed high-yield double-Z-pinch-driven hohlraum ICF configuration, but at the same physical scale, have been performed for the first time. The experiments, performed on Sandia National Laboratories's Z accelerator, represent the first ICF capsule implosions in a Z-pinch-driven hohlraum with a fixed wall. (Notably, this particular hohlraum configuration has the clearest path for meeting ignition-relevant symmetry requirements for pulsed-power systems [2,3].) Furthermore, the high-accuracy polar radiation symmetry measurement is the first in a pulsed-power-driven ICF configuration. When scaled from 70 to 220 eV, the radiation uniformity inferred from the capsule shell in the hohlraum geometry that was computer optimized to have optimum symmetry appeared to be within a factor of 1.6–4 of that required for ignition. An implosion imaged later in time indicated a capsule-convergence ratio of $\mathrm{Cr} = 14$–21. Although the secondary hohlraum geometry was deliberately not the optimum in this case, the Cr attained is the highest yet demonstrated in any pulsed-power-driven ICF system.

The authors thank the Z and ZBL operations teams for technical support. Sandia is a multiprogram laboratory operated by Sandia Corporation, a Lockheed Martin Company, for the U.S. Department of Energy under Contract No. DE-AC04-94AL85000.

[1] J. Lindl, *Inertial Confinement Fusion* (Springer-Verlag, New York, 1998).
[2] J. H. Hammer *et al.*, Phys. Plasmas **6**, 2129 (1999).
[3] M. E. Cuneo *et al.*, Phys. Rev. Lett. **88**, 215004 (2002).
[4] M. E. Cuneo *et al.*, Phys. Plasmas **8**, 2257 (2001).
[5] M. E. Cuneo *et al.*, Laser Part. Beams **19**, 481 (2001).
[6] R. B. Spielman *et al.*, Phys. Plasmas **5**, 2105 (1998).
[7] $\langle \Delta I \rangle / I$ is the time-averaged drive asymmetry applied to a capsule. I is the drive flux averaged over the capsule surface, and $\langle \Delta I \rangle = [(I_{\max} - I) + (I - I_{\min})]/2$.
[8] This quantity includes a 8/7 adjustment compared with normal usage because $\langle \Delta I \rangle / I$, strictly speaking, does not replace the pressure asymmetry $\langle \Delta P \rangle / P$, since $\langle \Delta P \rangle / P = (7/8) \langle \Delta I \rangle / I$. This relation arises because, for low-Z ablators, the pressure is related to the radiation temperature (T) by $P \sim T^{3.5}$ [1], whereas from Stefan-Boltzmann $I \sim T^4$. Thus, $P \sim I^{3.5/4}$, implying $dP/P = (7/8) dI/I$.
[9] R. A. Vesey *et al.*, Bull. Am. Phys. Soc. **43**, 1903 (1998); **44**, 227 (1999); **45**, 360 (2000).
[10] R. A. Vesey *et al.*, in *Proceedings of the International Conference on Fusion Science and Applications (IFSA2001), Kyoto, 2001*, edited by K. A. Tanaka, D. D. Meyerhofer, and J. Meyer-ter-Vehn (Elsevier, Paris, 2002), p. 681.
[11] D. L. Hanson *et al.*, Phys. Plasmas **9**, 2173 (2002).
[12] G. R. Bennett *et al.*, Rev. Sci. Instrum. **72**, 657 (2001).
[13] S. M. Pollaine *et al.*, Phys. Plasmas **8**, 2357 (2001).
[14] G. B. Zimmerman and W. L. Kruer, Comments Plasma Phys. Control. Fusion **2**, 51 (1975).
[15] $\langle \Delta r \rangle / r$ is the instantaneous level of capsule shell distortion from sphericity. r is the radius of a sphere having the same volume as the distorted capsule, and $\langle \Delta r \rangle = [(r_{\max} - r) + (r - r_{\min})]/2$.
[16] G. R. Bennett, Appl. Opt. **40**, 4570 (2001).
[17] G. R. Bennett and J. A. Folta, Appl. Opt. **40**, 4588 (2001).